Estimating Increased Sediment Loads Following Wildfire: Sampling Strategies and Stochastic Uncertainty

Sheridan, G.J[1, 2, 3], P.N.J. Lane[1, 2, 3], C.B. Sherwin[1] and P.J. Noske[1]

[1]School of Forest and Ecosystem Science, The University of Melbourne, Victoria
[2]eWater Cooperative Research Centre
[3]Cooperative Research Centre for Forestry
Email: sheridan@unimelb.edu.au

Keywords: *fire, water quality, soil erosion, Monte Carlo, forests, bushfire*

EXTENDED ABSTRACT

Severe wildfire swept through north-eastern Victoria, Australia, in early 2003 burning approximately 1.3 million ha including the catchments of major water impoundments such as the Gippsland Lakes, and the Hume and Dartmouth dams. There were immediate requests from catchment managers and water authorities for estimates of likely water quality impacts. In response, the Victorian Department of Sustainability and Environment commissioned a number of stage triggered automatic water quality samplers to be placed at existing hydrologic stations within catchments to the north and south of the Great Dividing Range, including the Ovens, Kiewa, Upper Murray, Snowy, Tambo, and Mitchell River basins. Only monitoring locations with a substantial pre-fire water quality monitoring history were selected. Sampling strategies prior to the fire were typically fixed interval manual monthly samples with between 10 and 30 years of sampling record. The objectives of this study were to: (i) quantify the change in total suspended sediment (TSS) loads following the fire, and; (ii) estimate the uncertainty surrounding those changes.

In an ideal world the pre and post treatment (i.e. fire) sampling strategies would be identical. This was not possible in this case, (or desirable, given the legacy dataset) and an optimal load estimation method was developed in response to the pre-existing sampling strategy. The linear interpolation method could not be applied to the post-fire dataset due to an incomplete event sampling record. Regression methods could not be applied because the relationship between flow and concentration was poor. Of the remaining options, the averaging method was selected as it could be applied to the pre and post datasets. To minimise the bias resulting from the post fire event based sampling strategy, the entire pre and post fire data were stratified into event and base flow categories using hydrograph analysis.

The uncertainty in estimated loads is rarely reported in the literature and this paper follows on from Etchells *et al.* (2005) by explicit reference to 3 broad error groupings:

1. *Measurement uncertainty,* associated with errors in measurement and sampling.
2. *Knowledge uncertainty,* involving our uncertainty in the process/model.
3. *Stochastic uncertainty,* due to variation in the data. Can be represented by the variance.

Measurement uncertainty was minimised by selection of the best load estimation method to match the available data. Knowledge uncertainty was evaluated to some extent by comparison of different load estimation methods for a subset of the data. Stochastic uncertainty was quantified using error calculations and through the use of Monte Carlo simulations.

The estimated increases in sediment loads for the year after the fire were large both in magnitude and variability between sites (from 20 to ≥ 1000 fold difference in pre- and post-fire loads). The majority of the total load was associated with event flows. Stochastic uncertainty was very large, with the standard deviation of the factor increases (over the pre fire state) being typically many times greater than the factor increase itself. Alternative load estimation methods produced values that varied by up to a factor of three. This uncertainty often resulted from a small number of extremely high sediment concentration values. The results indicate that the effects of fires on water quality are likely to be very large, and that increasing the precision of load estimates following future fires will require a much more intensive sampling strategy.

1. INTRODUCTION

Elevated post-fire sediment loads are widely recognised as a consequence of intense wildfire, however the magnitude of these increases has rarely been quantified in Australia. This paucity of data means there is little knowledge of the possible scale and longevity of impacts, and no parameters with which to populate water quality models.

A key aspect is the estimation of uncertainty around load estimates which is rarely presented in water quality studies. This paper explores the issues and uncertainty associated with estimation of pre- and post-fire suspended sediment loads and derivation of meaningful water quality model parameter values from sub-optimal sampling regimes.

2. STUDY SITES

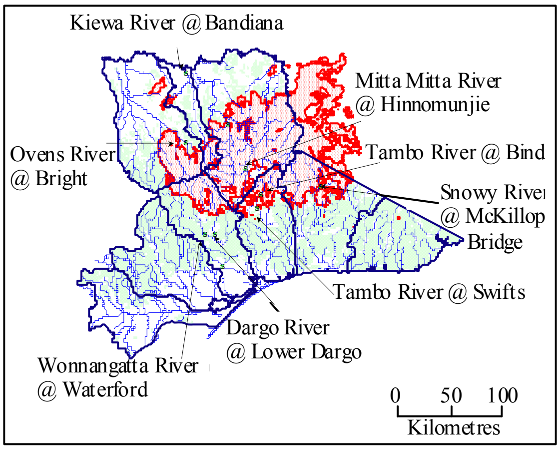

Figure 1. Location of the monitoring stations in NE Victoria. The red hatching is the burnt area.

The locations of monitoring stations are shown in Figure 1. Only data from three stations will be discussed in this paper; Dargo River (672 km^2), Mitta Mitta River (1533 km^2), and 2 stations on the Tambo River, Bindi (523 km^2) and Swifts Creek (943 km^2). These catchments had the best coverage of samples. Unfortunately, several sites had issues with auto-samplers not triggering during storms resulting in incomplete data sets. For these catchments, the issues surrounding uncertainty pertinent to the Dargo, Tambo and Mitta Mitta are multiplied.

3. UNCERTAINTY

The estimation of catchment exports of TSS and other constituents often include considerable uncertainty from a range of sources. There are a number of error taxonomies, however a simple classification listed by Etchells *et al.* (2005) includes 3 broad error groupings (see listing in the extended abstract).

Measurement uncertainty: For this study the measurement uncertainty is probably dominated by the temporal timing and frequency of the stream sampling regime, which differed between the pre-fire and post-fire period. The pre-fire samples were fixed interval (usually monthly) manual grab samples. A total of 150, 189, 35, and 196 pre-fire water quality samples were analysed for the Dargo River, Mitta Mitta River, Tambo River at Bindi, and Tambo River at Swifts Creek, respectively.

Post-fire water quality samples were collected by auto samplers, triggered by manual float switches during storm events. Figure 2 illustrates the post-fire event sampling regime, while Table 1 summarises the proportion of storms reasonably "captured" by the storm event triggered sampling.

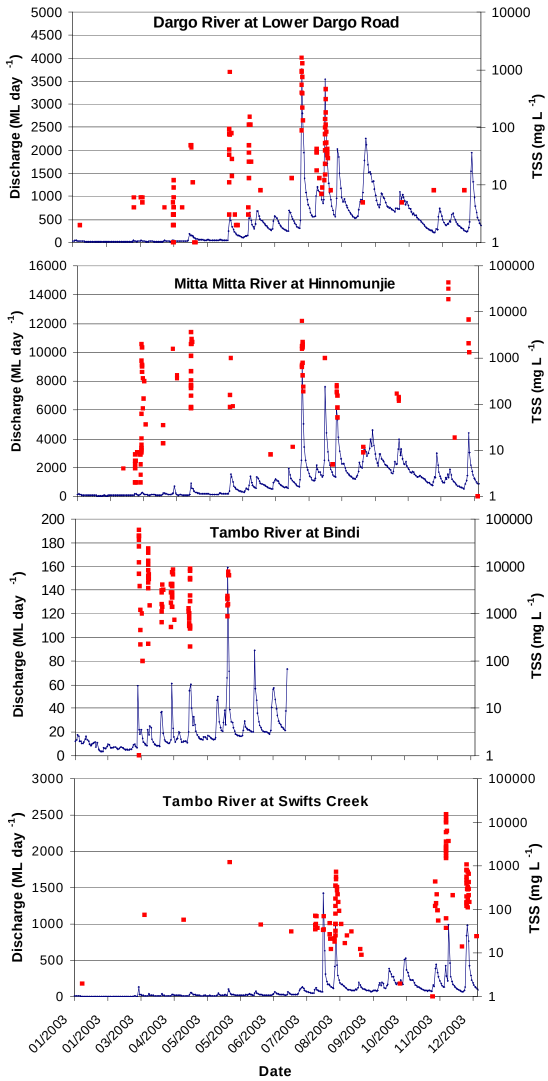

Figure 2. Daily discharge and TSS sample times and concentrations.

Table 1. A summary of the storm-event-based post fire sampling data, illustrating the degree to which storm events were captured by the auto-sampling regime.

Location	Total No of events	Num sampled	% sampled	Pre 2003 sampled
Dargo River	16	6	38	86
Mitta Mitta River	19	10	53	106
Tambo River at Bindi	8	6	75	10
Tambo River at Swifts Ck	17	5	29	107

Knowledge uncertainty: This source of uncertainty can be minimised by better understanding the processes that drive variation in loads, and by ensuring that the effects of these processes are represented within the model. This process representation and data availability drives model choice. Possible models for pollutant load estimation are described below.

The net load of in-stream TSS exported from the catchment S_t can be represented by the equation;

$$S_t = \int_0^T CQdt \qquad (1)$$

where C and Q are the instantaneous sediment concentration and discharge volume respectively, t is time, and t = T is the duration over which the load is calculated. An expression describing the product C·Q as a function of time is generally not available so S_t is approximated by;

$$S_t = \sum_{i=1}^{i=\frac{T}{t}} C_i Q_i \qquad (2)$$

where i is the interval number, and when the sampling interval t is short compared to the period of time over which the discharge and concentration vary. While discharge is often frequently recorded, concentration is not (except in the case of in-situ turbidity measurement) and linear interpolation is therefore used between points of measurement given by;

$$\sum_{i=1}^{n+1} \sum_{t_i < t \le t_{i+1}} q_t \frac{C_{t_i}(t_{i+1} - t) + C_{t_{i+1}}(t - t_i)}{t_{i+1} - t_i} \qquad (3)$$

where concentrations are denoted C_{t_i} , t_i i=1,…,n are the times at which concentration is measured, t_0 and t_{n+1} are the times at the start and end of each sub-interval, and q_t is the discharge at each timestep.

The problems associated with accurate estimation of sediment and nutrient loads are numerous. They include both the physical constraints of implementing appropriate sampling regimes, and the related statistical issues associated with load estimation (Etchells *et al.* 2005, Cohn 1995, Letcher *et al.* 1999, Preston *et al.* 1989). Equation 3 is often used to estimate the "true" load (Equation 1) from catchments. If the sampling interval is large compared to the period of time over which the discharge and concentration vary then use of Equation 3 will result in large errors. In this case alternative load estimation methods are required, which can be categorised into three broad classes (Preston *et al.* 1989);

1. Averaging
2. Ratio estimators
3. Regression methods (rating curves)

In an ideal world selection of a sampling strategy should follow from the selection of a load estimation method, however in reality water quality data is often scarce, and is collected for a variety of different purposes. In practice it is often necessary to select a load estimation method to best suit the available dataset, taking into consideration factors such as the frequency and length of period of sampling, and the type of sampling (eg. fixed interval vs storm event sampling). For example, fixed interval sampling over short study durations will tend to under represent the larger events, resulting in underestimates of the true load. Exploratory analysis of the water quality dataset is required to establish whether or not the assumptions associated with each load estimation method are violated. Ideally, an estimator should be precise (ie. have low variance) and accurate (low bias). An unbiased estimator has an expected value that is equal to the population parameter. Stratification (eg. by flow category, season, rising or falling limb of the hydrograph) of the data may also improve load estimates. Estimation methods are described in more detail below.

Averaging

A typical example of an averaging method for the estimation of the load L of a constituent is given by the model;

$$L = Q\sum_{i=1}^{n} \frac{c_i}{n} \qquad (4)$$

where Q is the total discharge, c_i is the concentration of the i^{th} sample, and n is the number of samples.

Ratio estimators

A typical example of a ratio estimator for the estimation of the load (L) of a constituent is given by a model where the average ratio of load to discharge is multiplied by the total discharge;

$$Y_R = (y/x)X \qquad (5)$$

where y and x are the sample means of load and discharge respectively, Y_R is the ratio estimate of load and X is the discharge. The ratio estimator is considered a best linear unbiased estimate under two conditions: The relation between the samples of load and discharge is a straight line through the origin, and the variance of the load samples is proportional to the discharge.

Monte Carlo Simulation

Monte Carlo simulation can be used with either the ratio or the averaging methods. The method involves generating a random population of input values from a theoretical distribution calculated from the observed data. Load estimates are made for each instance of the input data, generating a distribution of estimated loads.

Regression methods

Regression methods exploit the often strong relationship between discharge and concentration. Generally, log-log regressions are applied because flow and concentration are assumed to be described by a bi-variate log normal distribution. A common log-log model is given by;

$$\mathrm{Ln}(C) = a + b\mathrm{Ln}(Q) \qquad (6)$$

where Q is the discharge, C is the concentration, and a and b are regression parameters. The model includes calculable error within the range of the regression and unknown error due to extrapolation of the regression outside the range over which the regression was developed. Preliminary analysis of the data collected in this study showed a poor relationship between discharge and concentration (Figure 3) and as a consequence the regression method was not used for load estimation.

In this study, a stratified averaging and Monte Carlo method were used. Interpolation was not possible as all events were not sampled (Figure 2), and samples for a number of events were biased toward the rising limb of the hydrograph. Regression analyses were explored (Figure 3), but the variables were not well correlated over the data range.

Stratification was based on a base-flow separation, using the Lyne and Hollick (Nathan and McMahon, 1990) method. Each day of record was categorised as either base-flow or event-flow based on a threshold value of the daily base-flow index (BFI, the ratio of base-flow to total flow). (BFI>0.85 was categorised as base-flow). A cut-off value < 1.0 was used after visual inspection to accommodate flows that exceeded the automatically separated base-flow which would be unlikely to carry event-level concentration of sediment. The flow records were then used to assign water quality samples to event-flow or base flow categories. The resultant concentrations were then averaged to obtain dry weather concentrations (DWCs) and event mean concentrations (EMCs).

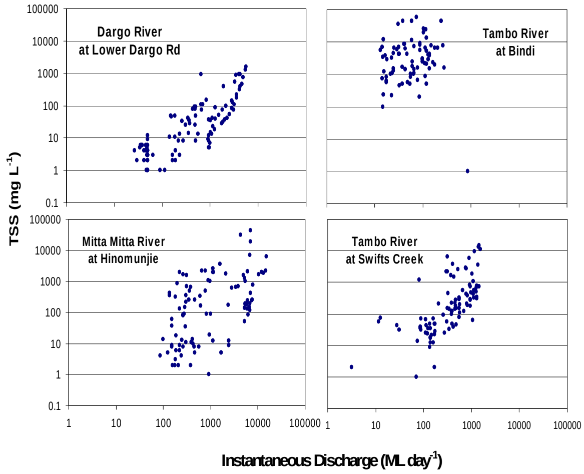

Figure 3. Instantaneous discharge and TSS concentration for the post-fire storm event triggered samples.

For the Monte Carlo simulation the same stratified (DWC, EMC) concentration data were used as for the averaging method. For each flow category at each site, the observed population of concentration values were assumed to be log-normal. The observed data for all the sites were assumed to be log-normal because: 1) for the sites with a large number of water quality samples, the sample distribution was observed to be approximately log-normal; 2) concentration data cannot be negative, and are often characterised by infrequent, very high concentration values, properties that are consistent with the log-normal distribution, and; 3) researchers commonly observe that water quality data is log-normally distributed (Parkhurst, 1998). Between 1000 and 60,000 random values with a log-normal distribution, the distribution parameters of the observed data were generated. The number of random values generated was determined by visually assessing a plot of sample size vs estimated mean, so as to determine the sensitivity of the sample parameters to the sample size. In general, observed samples with larger variances required a larger sample size to generate a stable mean value.

These concentration distributions were then multiplied by the appropriate discharge volume for each year in each flow strata at each site. The loads based on the DWC and the EMC were added at each iteration to get a total load for that iteration. This population of loads was the output from the simulation.

Finally, stochastic uncertainty reflects the underlying variability in the data, in this case sediment concentration data, which can be readily quantified using estimates of the variance. The analytical propagation of stochastic uncertainty through estimation models can become complex even with relatively simple models. The following sets out the uncertainty methods used.

Arithmetic Averaging

An important, but often neglected component of water quality analysis is error estimation. The error in load estimates using the averaging method were determined by applying the propagation of error formula for Y =f(X,Z, …);

$$s_y = \sqrt{\left(\frac{\partial Y}{\partial X}\right)^2 s_x^2 + \left(\frac{\partial Y}{\partial Z}\right)^2 s_z^2 + \ldots + \left(\frac{\partial Y}{\partial X}\right)\left(\frac{\partial Y}{\partial Z}\right) s_{xz}^2} \quad (3)$$

where s_x , s_z and s_y are the standard deviations of the *X, Z,* and *Y* measurements respectively, and

$\frac{\partial Y}{\partial X}$ is the partial derivative of the function *Y* with respect to *X.* s_{xz} is the estimated covariance between the *X,Z* measurements. The covariance term is zero if *X* and *Z* measurements are independent, and should be included only if estimated from sufficient data. Applying the propagation of error formula to the load estimation equation gives;

$$s_L = \sqrt{\left(\frac{\partial L}{\partial \overline{C}}\right)^2 s_C^2 + \left(\frac{\partial L}{\partial V}\right)^2 s_v^2 + \ldots + \left(\frac{\partial L}{\partial C}\right)\left(\frac{\partial L}{\partial V}\right) s_{CV}^2} \quad (4)$$

where s_C s_v and s_L are the standard deviation of the concentration volume and load measurements respectively. The partial derivatives simplify, giving $\frac{\partial L}{\partial \overline{C}} = V$ and $\frac{\partial L}{\partial V} = \overline{C}$. Assuming the covariance between V and $\overline{C}$ is zero (this is unknown due to the short time period of available data, but unlikely), Equation 4 simplifies to;

$$s_L = \sqrt{V^2 s_C^2 + \overline{C}^2 s_V^2} \quad (5)$$

which is in a form used by Hart *et al*. (1987) for estimating uncertainty in load estimates. In this study the volume measurement *V* is a single annual value at each site for the year of the load estimate (allocated proportionally to the base-flow and event flow categories based on the base-flow separation), and therefore the variance s_v^2 cannot be calculated. A coefficient of variation (C_v) of 10% for the volume estimate was assumed and the standard deviation s_v was subsequently approximated by transposing the coefficient of variation formula;

$$C_v = \frac{s_V}{V} * \frac{100}{1} \quad (6)$$

The standard deviation s_L of the load estimate is calculated for each of the two flow categories (event flow L_1, and dry weather flow, L_2) and combined by;

$$s_L = \sqrt{s_{L_1}^2 + s_{L_2}^2} \quad (7)$$

to give the standard deviation of the estimated total load. The uncertainty in the ratio of the absolute values of predicted post-fire (Bt) and pre-fire (UnBt) load (ie. the factor change) is approximated from (Hepworth *pers comm.*);

$$\mathrm{var}(Bt/UnBt) = \frac{\mathrm{var}(Bt)/[E(UnBt)]^2 + \mathrm{var}(UnBt)[E(Bt)]^2}{[E(UnBt)]^4 v} \quad (8)$$

This approximation is calculated using the delta method, by expanding the function f(x,y) = x/y in a Taylor series around the mean value (E(X), E(Y)) and taking the variance of the linear terms. There are more terms in the series, though they don't contribute significantly to the estimated variance in the ratio. Note that the covariance is assumed to be zero in this approximation.

Monte Carlo simulation

The expected value E(X) and variance var(X) of the observed data was determined, respectively, from;

$$E(X) = \exp(\mu + \frac{\sigma^2}{2}) \quad (9)$$

$$\mathrm{var}(X) = (\exp(\sigma^2) - 1)\exp(2\mu + \sigma^2) \quad (10)$$

Where μ and σ are the mean and standard deviation of the logarithms of the observed data.

4. ESTIMATION AND UNCERTAINTY RESULTS

Estimated loads, factor increases and uncertainties for both the arithmetic method and the arithmetic method using Monte Carlo simulation are given in Table 2.

Four aspects are immediately obvious;

1. The large magnitude of the load increases
2. The very high variability between catchments
3. The very high *stochastic uncertainty* on the estimates of loads. In many cases the standard deviation of the estimated load is greater than the mean value. *Measurement uncertainty* due to sampling error is additional to the listed error values.
4. The variation in estimated loads depending on the load estimation method used (eg. arithmetic mean vs Monte Carlo simulation using the averaging method), particularly when the data are strongly skewed and affected by extreme values.

Table 2. Estimated TSS loads, factor increases and uncertainties.

		Arithmetic Method										Monte Carlo Method					
Catchment	Year	Baseflow Conc. (mg L^{-1})	Eventflow Conc. (mg L^{-1})	Unburnt Total Load (tonnes)	Unburnt SD	Burnt Total Load (tonnes)	Burnt SD	Unburnt (tonnes $km^{-2}yr^{-1}$)	Burnt (tonnes $km^{-2}yr^{-1}$)	Relative Change	SD of Relative Change	Unburnt Total Load (tonnes)	Unburnt SD	Burnt Total Load (tonnes)	Burnt SD	Relative Change	SD of Relative Change
Tambo @ Swifts	Unburnt	4.10	5.75														
Tambo @ Swifts	Burnt03	26.50	1139.07	193	502	32967	77586	0.2156	36.83	171	600	145	150	33443	146511	230	1036
Tambo @ Bindi	Unburnt	3.13	4.50														
Tambo @ Bindi	Burnt03	2662.00	7069.84	17	6	24147	35811	0.0316	46.20	1459	2165	18	14	26103	40333	1462	2534
Dargo	Unburnt	3.30	4.62														
Dargo	Burnt03	6.67	119.66	701	600	14854	33714	1.0376	21.97	21	51	646	509	13692	69116	21	108
Mitta Mitta	Unburnt	2.86	9.35														
Mitta Mitta	Burnt03	101.90	1721.10	3037	1409	511559	1716019	1.9812	333.70	168	570	2279	3125	817192	6087376	359	2716

Although the uncertainty estimation around the load increases are very high, the results suggest there was a very significant increase in loads. The concentration data alone (Figure 2 and Table 1) demonstrates this large increase. The variability of impacts is most likely to be a function of the severity of the burn and rate of subsequent vegetation recovery; the intensity and volume of rainfall following the fires; and the interaction of these factors. Additionally, differences in response may reflect the proximity of the monitoring stations to the burnt area; the total percentage of catchment burnt; and the degree to which riparian areas were impacted.

The large uncertainties and variation in loads produced from the analyses beg the question of the sensitivity of the results to the selected load estimation method. A further exploration of the data from one catchment (Tambo River at Bindi) was undertaken. Data from the first 6 months after the fire was used as the sampling regime was the most complete of all the data sets. Seven methods were used to estimate loads, including regression against discharge, linear interpolation, Monte Carlo, and 4 variations on the averaging method considering non-stratified and stratified estimation, and use of geometric and arithmetic means for the stratified and non-stratified cases.

Table 3 shows that estimates varied about three-fold depending on the load estimation method used, from around 5000t to around 15,000t. Methods using the geometric mean produce results most similar to the interpolation method, while methods using the arithmetic mean, or the Monte Carlo simulation produce estimates at the high end of the range. Parkhurst (1998) suggests that for concentration data where mass balances are being calculated that the arithmetic mean is in most cases superior, except perhaps where the number of samples is low (eg. N < 5), in which case the geometric mean may be superior.

Table 3. Comparison of loads (t) using a range of different load estimation methods.

Method	Discharge (ML)			Concentration (mg/L)			Load (t)		
	Total	% base	% event	All data	Base only	Event only	Total	% base	% event
Regression	<< method could not be applied >>								
Linear interpolation	2,314	--	--	--	--	--	4,803	--	--
Arithmetic mean	2,314	--	--	6,798	--	--	15,732	--	--
Geometric mean	2,314	--	--	2,852	--	--	6,600	--	--
Arithmetic mean stratified	2,314	21	79	--	2,662	6,978	14,050	9	91
Geometric mean stratified	2,314	21	79	--	2,110	2,909	6,343	16	84
Monte Carlo stratified		21	79	--	--	--	Approx 15,000	10	90

Unfortunately, it is difficult to conclude which method is "best" from this analysis, because the interpolation method could not be applied with a high degree of certainty. It should also be noted that the "best" method for this site may not be the best method for a different catchment with different data properties. However, the analysis does give an indication of the possible range in estimated loads when the input data is relatively good.

5. DISCUSSION

The results of the various load estimation has demonstrated the very significant water quality impacts that can be generated by fire, and the equally significant issues associated with uncertainty around the estimate. These uncertainty estimates are rarely given in water quality studies. The stochastic uncertainty is particularly high with data such as this due to the very high concentrations that are generated post-fire, resulting in large standard deviations.

Where water quality models are parameterised by data such as this, the uncertainty surrounding predictions are very significant. The EMCs and DWCs were used by Feikema *et al.* (2005) to parameterise the E2 model for prediction of TSS, total phosphorous and total nitrogen downstream of the hydrologic stations depicted in Figure 1. Feikema *et al.* (2005) noted that the uncertainties around those predictions are large, with a large proportion of this uncertainty due to the uncertainty in the estimation of EMC and DWC values.

The results indicate that increasing the precision of load estimates following high-disturbance events such as wildfire will require a substantially more intensive sampling strategy in future. For example, Lane *et al.* (2006) obtained error estimates for TSS loads of < 10% using 15 minute turbidity observations and the regression method for load estimation. However this approach carries considerable maintenance overheads, with equipment requiring frequent calibration, and would be costly to apply in the remote locations reported in this study.

6. ACKNOWLEDGMENTS

The authors would like to thank the Victorian Department of Sustainability and Environment for funding this study.

7. REFERENCES

Cohn TA (1995), Recent advances in statistical methods for the estimation of sediment and nutrient transport in rivers. *Reviews of Geophysics,* 33, 1117-1123.

Etchells T, Tan KS and Fox DR (2005), Quantifying the uncertainty of nutrient estimates in the Shepparton Irrigation Region In Zerger, A. and Argent, R.M. (eds) MODSIM 2005 International Congress on Modelling and Simulation. Modelling and Simulation Society of Australia and New Zealand, December 2005, 2755-2761. ISBN: 0-9758400-2-9.

Feikema, P.M., G.J. Sheridan, R.M. Argent, P.N.J. Lane and R.B. Grayson (2005), Using E2 to Model The Impacts Of Bushfires On Water Quality In South-Eastern Australia. In Zerger, A. and Argent, R.M. (eds) MODSIM 2005 International Congress on Modelling and Simulation. Modelling and Simulation Society of Australia and New Zealand, December 2005, pp. 170-176. ISBN: 0-9758400-2-9.

Hart BT, Ottaway EM, And Noller BN (1987), Magela Creek system, northern Australia, II. Material budget for the floodplain. *Australian Journal of Marine and Freshwater Research.* 38, 861-876.

Hepworth G. (pers comm.) Statistical Consulting Centre. The University of Melbourne.

Lane, P.N.J., Sheridan, G.J. and Noske, P.J. (2006), Changes in sediment loads and discharge from small mountain catchments following wildfire in south eastern Australia. *Journal of Hydrology*, 331, 495-510

Letcher RA, Jakeman AJ, Merrit WS, McKee LJ, Eyre BD, Baginska B (1999), A review of techniques to estimate catchment exports. EPA NSW Technical Report, 110.

Nathan, R.J. and McMahon, T.A. (1990), Evaluation of automated techniques for base-flow and recession analysis. *Water Resource Research* 26(7), 1465-1473.

Parkhurst, D. (1998), Arithmetic versus geometric means for environmental concentration data. *Environmental Science and Technology* 32 (3) pp92-98.

Preston SD, Bierman Jr VJ, Silliman SE. (1989), An evaluation of methods for the estimation of tributary mass loads. *Water Resources Research* 25 (6): 1379-1389.